Zagazig University Medical Journal
www.zumj.journals.ekb.eg
https://doi.org/10.21608/zumj.2024.262202.3110 Volume 30, Issue 8.1, NOV. 2024, Supplement Issue

Manuscript id: ZUMJ-2401-3110
Doi: 10.21608/ZUMJ.2024.262202.3110

ORIGINAL ARTICLE

Role of MR-CSF Flowmetry in Diagnosis and Differentiation of ventriculomegaly

Norhan Mohamed Helmy[1*], Faten Fawzy Mohammed Hafez[1], Mohamed Ashraf Zaitoun[1], Riham Dessouky[1]

[1] Radiodiagnosis Department, Faculty of Medicine, Zagazig University, Zagazig, Egypt.

*** Corresponding author:**
Norhan Mohamed Helmy
Email:
helmynoran@gmail.com

Submit Date:12-01-2024
Revise Date: 26-01-2024
Accept Date: 03-02-2024

ABSTRACT

Background: Hydrocephalus is the buildup of fluid within the brain's ventricular system due to disturbance of cerebrospinal fluid (CSF) formation, flow, or absorption. The excess CSF associated with hydrocephalus can cause a range of functional cerebral disorders. This study aims to assess the role of CSF flowmetry in the diagnosis and differentiation between different causes of ventriculomegaly.

Methods: This cross-sectional study was performed on 46 patients, 36 cases divided into four subgroups based on their clinical and MRI findings as follows: Normal pressure Hydrocephalus (NPH) group, aqueductal stenosis group, atrophic changes (related to aging) group, other neurological diseases group; subdivided into ventriculoperitoneal (VP) shunt, Chiari malformation type I, and evacodilatation (caused by brain tissue volume loss rather than intraventricular tumor) secondary to the treated tumor. Moreover, the final group consisted of 10 patients free from any medical disease or radiological finding and were considered the control group; all cases were subjected to complete history taking, clinical examination, MR, and CSF flowmetry examination.

Results: On comparison between aqueductal stenosis and control groups respecting the comparative age of the control group, there was a substantial variance between groups with regards to Evan's index, SV, PSV, and EDV (p-values= 0.012, 0.003, 0.001, and 0.024, respectively). All values were significantly higher in the aqueduct stenosis group. The best cutoff of SV in the diagnosis of atrophic neurological lesions versus NPH was ≤44.5 µL/cycle with the area under curve 0.923 with an overall accuracy of 91.3% ($p<0.001$).

Conclusion: CSF flowmetry is a reliable, comprehensive technique for the localization of level of obstruction, differentiation between brain atrophic changes and NPH, evaluation of VP shunt function, shunt responsiveness, and objective follow-up of different neurological diseases due to its high predictive value by which we can evaluate clinical course prior to and after surgery.

Keywords: cerebrospinal fluid, CSF flowmetry, ventriculomegaly.

INTRODUCTION

Hydrocephalus is the buildup of fluid within the ventricular system of the brain due to disturbance in cerebrospinal fluid (CSF) formation, flow, or absorption. The excess CSF correlated with hydrocephalus can harm cerebral tissue and cause a range of functional cerebral disorders, which may vary according to patient age and general condition [1].

Magnetic resonance imaging (MRI) CSF flowmetry has various clinical applications in hydrocephalic patients. Initially, it can distinguish between kinds that communicate and those that do not by properly localizing the obstruction site. Secondly, in patients with Chiari and Dandy-Walker abnormalities, it can precisely evaluate arachnoid cysts and determine the change in CSF movement. Moreover, hydrocephalus and ventriculomegaly secondary to

evacuodilatation can be differentiated, also discriminates syringomyelia from cystic myelomalacia, evaluates flow patterns of posterior fossa cystic malformations, and evaluates aqueductal patency. In addition, it is feasible to evaluate shunt surgeries as well as interventional techniques like aqueductoplasty and endoscopic third ventriculostomy [2].

Phase contrast MRI is a quick, simple-to-utilize, non-invasive method that can assess CSF flow both quantitatively and qualitatively. It is sensitive to even minimal CSF flows. Cine phase-contrast MR images permit the identification of obstruction if present in any segment of the CSF conduit. They do this by displaying CSF flow in a dynamic, easily discernible, and more attractive manner. CSF flow evaluation at the anticipated level of obstruction provides repeatable and dependable results for a more accurate diagnosis. It can also be used to inform therapy choices and more reliably monitor treatment effects [3,4].

Over the past twenty years, there has been a growing application of flow-sensitive MRI techniques to evaluate CSF flow dynamics both quantitatively and qualitatively [2]. Axial and sagittal images are used for Phase Contrast MRI procedures. The craniocaudal direction of axial plane images enables flow quantification, while the craniocaudal direction of sagittal images enables qualitative assessment [8]. Furthermore, Cine phase CSF flowmetry parameters can even detect flow anomalies in patients with normal CSF pressure [5].

The present work is designed for the assessment of the role of CSF flowmetry in the diagnosis and differentiation between different causes of ventriculomegaly.

METHODS

Patients

This cross-sectional study was carried out from December 2022 till June 2023 at the Radio-diagnosis Department, Faculty of Medicine, Zagazig University, and other institutes to obtain a representative variety of cases. Patients included in our study were referred from the neurology department. Our IRB-approved study protocol included a sample size of 6 cases/per month for six months. Furthermore, we included ten control cases, i.e., healthy volunteers, in addition to the 36 cases. All patients were included in a consecutive order to ensure the integrity of the findings and results. Forty-six cases were enrolled in the study, 21 females and 25 males, aged between 10 months and 88 years, of both sexes. Verbal and written informed consent was obtained from all participants after an explanation of the procedure and medical research. The research was conducted under the World Medical Association's Code of Ethics (Helsinki Declaration) for human research. This study was carried out after the approval of the Institutional Review Board (IRB#10068/2-11-2022).

Our final sample size included 46 cases; 36 patients divided into four subgroups based on their clinical & MRI findings as follows: - Normal Pressure Hydrocephalus (NPH) group, aqueductal stenosis group, atrophic changes (related to aging) group, other neurological diseases group subdivided into ventriculoperitoneal (VP) shunt, Chiari malformation type I, and evacodilatation (secondary to the tumor). The final group consisted of 10 cases that were free from any medical disease or radiological finding and were considered the control group.

Cases with the following criteria were included: all patients with clinically suspected hydrocephalus, ventriculomegaly in different age groups (Evans' index > 0.3), and patients undergoing VP shunt operation.

Cases with the following characteristics were excluded: clinically unstable patients with cofounding meningitis and absolute contraindications to MRI as cardiac pacemakers, drug infusion pumps, cochlear implants, and implantable neurostimulation devices.

Methods

Patient population

After re-interviewing the adult patients and parents of all participating children and reviewing the goal and end points of the study, all patients were subjected to Complete history taking, clinical examination, MR, and CSF flowmetry examination.

Technique

Patient preparation: On arrival at the MRI unit, patients were re-interviewed to exclude any contraindications to performing the MRI examination. Irritable or uncooperative patients (mostly infants, children, or irritable adults) were referred to an attending anesthesiologist for sedation. Premedication used during sedation was Ketamine 3 mg/Kg IM and Atropine 0.01 mg/kg

(for adults) or Choral hydrate 250 mg orally (for children ages 7 to 12 years old).

MRI data acquisition: All studies were carried out on 1.5 tesla MRI machines as follows: Philips Achieva DS 2019, GE Explorer 2018, and Siemens MAGNETOM Altea 2018 that were used according to institutional availability. Placement of magnet compatible ECG leads was performed for cardiac gating. The patient was laid down on the MRI table in supine position following placement of the head coil.

All participants got routine brain MRI, including:

- ***Axial T1WIs:*** TE =10 ms, TR = 538 ms. and additional sagittal T2WIs.
- ***Axial T2WIs :*** TE =120 ms, TR =4130.
- ***Axial FLAIR:*** TR= 11000 ms, TE = 140 ms, TI =2800 ms.
- ***Axial DWI :*** TR = 3700 ms, TE = 108 ms.

The standard brain MRI routine was supplemented with a phase contrast MRI run for each subject. Electrocardiography (ECG) results in frames that capture the full cardiac cycle, or a peripheral pulse unit (PPU) is used to gate phase contrast MRI to the cardiac cycle. When available, ECG gating was always preferably used; however, since quantitative measurements mainly rely on systolic and diastolic variability to plot curves, PPU was considered an acceptable alternative. The sagittal and axial phase contrast MRI were carried out using the following acquisition parameters:

- ***Flip angle:*** 10 degrees.
- TR and TE: 21 and 6.8, respectively
- ***Slice thickness:*** 10 mm.
- ***FOV:*** 190 mm.
- ***Matrix size:*** 236 x 182 pixels.
- ***Encoding velocity:*** 8-12 cm/s (differed respecting to expected velocity in each case).
- ***Encoding direction:*** cranio-caudal or caudo-cranial (depending on velocity encoding direction).

At the end of the procedure, the head coil was removed, and sedated patients stayed under the observation of the anesthesiologist until they regained consciousness.

Data collection

Images were transferred from the scanner console to a dedicated workstation. Two radiologists (with 4 and 14 years of experience) analyzed anatomic images in consensus and checked velocity curves to ensure the reliability of quantitative measures. Phase contrast qualitative MR images were examined for atypical flow patterns, including simultaneous bidirectional flow, signal inhomogeneity, and attenuated flow. The following quantitative parameters were examined in a series of phase and magnitude images acquired at the systolic and diastolic phases of the cardiac cycle: peak systolic velocity (PSV) in cm/sec, stroke volume (SV) in microliter µL /cycle, and end-diastolic velocity (EDV) in cm/sec (G in figs 1 and 2). Results were compared with normal values.

Since different scanners according to institutional availability to achieve adequate sample size and include various neurologic diseases, we avoided variability or miscalculation among software by performed a semiautomatic calculation of quantitative parameters (only absolute flow values were obtained directly from the scanner) using the following equations.

a) Philips scanner: Stroke Volume (SV) (in µL /cycle) = (Forward flow volume (in ml/sec) x 1000 + backward flow volume (in ml/sec) x 1000) / 2.

b) GE scanner: Stroke volume (SV) (in µL /cycle) = mean systolic flow (calculated as the sum of flux values/number of phases) x duration of the cardiac cycle.

c) Siemens scanner: Stroke volume (SV) (in µL /cycle) = mean systolic flow (calculated as the sum of flux values/number of phases) x duration of the cardiac cycle.

STATISTICAL ANALYSIS

Data were analyzed utilizing Statistics Package for Social Sciences (SPSS) version 26. Absolute frequencies of categorical variables were used to define them, and the chi-square test and, when suitable, the Fisher exact test were used for comparison. Using chi-square for the trend test, ordinal data between the two groups was compared. Assumptions utilized in parametric testing were checked using the Shapiro-Wilk test. Depending on the data type, quantitative variables were described using mean, standard deviations, median, and interquartile range.

The independent sample t-test and the Mann-Whitney test were used to compare quantitative data between two (each disease and control) groups (tables 2, 3, and 4) depending on whether the data was regularly distributed or not. One-way ANOVA and Kruskal-Wallis tests were used was to compare all patient groups (Table 5). The ROC curve analysis was employed to identify the optimal cutoff of specific quantitative characteristics for the

diagnosis of a particular health issue. P<0.05 is considered significant.

RESULTS

Patient population

Of the patient population, (25) 54.3 % were males and (21) 45.7% were females. The control group included 10 cases with ages ranging from 11 - 64 years; of the control group population, 60% were males, and 40 % were female. Patients were categorized as 36 patients with neurological lesions and 10 cases with no neurological lesions.

Image interpretation:

Lesions were distributed as 28.3% with NPH, 21.7% with atrophic changes, 15.2% with aqueduct stenosis, 4.3% with Chiari malformations, 4.3 % with a previous VP shunt, and 4.3% with evacodilatation due to the treated tumor. On conventional MRI imaging, ventricular dilatation was the main finding in all included cases, with specific findings for each disease that are summarized in (Table 1) of the MRI findings of the diseased patient groups.

On comparison between atrophic change (age range 54 - 88 years) and control group (age range 37 - 64 years), there was a substantial variance between groups with regards to Evan's index and SV (p <0.05). Despite higher stroke volume in the atrophic change group, these values remained lower than other neurological disorders (Figure 2, Table 2).

On comparison between the NPH group (age range 39 - 81 years) and control group (age range 37-64 years), there was a marked variance between groups with regards to Evan's index, SV, PSV, and EDV (p<0.05). All values were significantly higher in the NPH group (Figure 1, Table 3).

On comparison between aqueductal stenosis (with age ranging from 10 - 58 years) and control groups respecting the comparative age of the control group, there was a notable variation between groups with regards to Evan's index, SV, PSV, and EDV (p<0.05). All values were remarkably increased in the aqueduct stenosis group (Table 4).

In comparison of all patient groups, there was a substantial variation between the studied groups concerning PSV (p-value=0.013). On pairwise comparison, there was a significantly lower difference in PSV in the atrophic changes group than in other groups. There was also a substantial variance between the studied groups respecting SV (p-value<0.001). In the pairwise comparison, the variance was substantial between the groups with atrophic changes and both aqueduct stenosis and NPH (Table 5).

On ROC curve analysis comparing NPH and atrophic changes, the best cutoff of SV in the diagnosis of atrophic neurological lesions versus NPH was ≤44.5 µL/cycle with the area under curve 0.923 and an overall accuracy of 91.3% (p<0.001) (Figure S1).

NPH patients are characterized by a triad of dementia (100 %), gait disturbance (100%), and urinary incontinence (69.2%). Brain atrophy patients clinically presented mainly with dementia (100 %) and headache (80 %). The other different neurological diseases, including Aqueductal stenosis, Chiari malformation type I, previously VP shunt, and evacodilatation of the treated tumor, had common symptoms such as headache, gait disturbance, and signs of delayed mental development in child patients. On clinical examination, most cases of different neurological diseases had signs of increased ICT (69.4 %) (Tables S1-S4).

Table 1: Demographic data of controls and studied patients, distribution of neurologic lesions, and conventional MRI in each patient

All Studied Cases	n=46 / Mean ± SD	% / range
Gender **Male** **Female**	 25 21	 54.3 % 45.7%
patient group	**n=36 / Mean ± SD**	**% / range**
Age (year)	46.2 ± 22.41	Ten months – 88 year
Gender: **Male** **Female**	 20 16	 55.6% 44.4%
Control cases	**n=10 / Mean ± SD**	**% / range**
Age (year)	36.5 ± 22.41	11-year - 46 year

All Studied Cases	n=46 / Mean ± SD	% / range
Gender: **Male** **Female**	 6 4	 60% 40%
Neurological lesions		
Diseased group NPH Atrophic changes Aqueduct stenosis Chiari malformation VP shunt Evacodilatation due to tumor **Control group**	 13 10 7 2 2 2 10	 28.3% 21.7% 15.2% 4.3% 4.3% 4.3% 21.7%
MRI findings		
1- NPH (N. = 13)	-Evan index > 0.3 (N.= 13). -Ventricular dilatation (N.=13) -Enlarged subarachnoid space disproportion to ventriculomegaly (N.=10). -empty sella (N.= 10).	
2-Atrophic changes (N. = 10)	-Prominent cortical sulci, basal cisterns, both Sylvian fissures and extra-axial CSF spaces with Ventricular system dilatation	
3-Aqueductal stenosis (N. = 7)	- Supratentorial hydrocephalus (often enlargement of both lateral ventricle & 3rd ventricle with relatively normal size 4th ventricle) (N.=7). -Aqueductal flow void sign / aqueductal web. (N.= 7)	
4- Chiari Malformation Type I (N.= 2)	-Herniation of cerebellar tonsils beyond foramen magnum (N.= 2). -Tonsils are pointed more than rounded (peg-like). (N.=2)	
5- Tumor (therapeutic SOL) (N. = 2).	-post-therapeutic changes: Evacodilatation of the ipsilateral ventricle (N.= 2).	
6- VP shunt (N.= 2)	-Ventricular dilatation with VP shunt inserted within ventricular system	

NPH: Normal pressure hydrocephalus, VP: ventriculoperitoneal.

Table 2: Comparison between the studied groups (atrophic changes and control group) regarding MR-CSF Flowmetry

	Atrophic changes	**Control group**	**T**	**p-value**
	Mean ± SD	**Mean ± SD**		
Evan's index	0.34 ± 0.07	0.29 ± 0.01	3.504	0.012*
	Median (IQR)	**Median (IQR)**	**Z-score**	**p-value**
PSV cm/sec	2.6(1.28 – 4.63)	3.5(2.35 – 3.88)	-0.605	0.545
EDV cm/sec	2.8(1.63 – 4.8)	3.2(2.96 – 3.73)	-0.608	0.543
SV µL /cycle	35.5 (28 – 38.25)	21(17.5 – 22.5)	-3.787	<0.001**

PSV: peak systolic velocity, EDV: end-diastolic velocity, SV: stroke volume

Table 3: Comparison between the studied groups (NPH and control group) regarding MR-CSF Flowmetry

	NPH (n=13)	Control group (n=10)	T	p-value
	Mean ± SD	Mean ± SD		
Evan's index	0.37 ± 0.08	0.29 ± 0.01	3.343	0.006*
SV µL /cycle	84.38 ± 33.48	20.6 ± 3.24	6.828	<0.001**
	Median (IQR)	Median (IQR)	Z-score	p-value
PSV cm/sec	5.8(3.94 – 8.12)	3.55(2.35 – 3.88)	-3.35	0.001**
EDV cm/sec	6.16(3.25 – 8.05)	3.2(2.96 – 3.73)	-2.115	0.034*

PSV: peak systolic velocity, EDV: end-diastolic velocity, SV: stroke volume

Table 4: Comparison between the studied groups (aqueductal stenosis and control group) regarding MR-CSF Flowmetry

	Aqueduct stenosis	Control group	t	p-value
	Mean ± SD	Mean ± SD		
Evan's index	0.42 ± 0.1	0.29 ± 0.01	3.504	0.012*
SV µL /cycle	117.43 ± 51.82	20.6 ± 3.24	4.937	0.003*
	Median(IQR)	Median(IQR)	Z -score	p-value
PSV cm/sec	5.74(4.7 – 9.5)	3.55(2.35 – 3.88)	-3.42	0.001**
EDV cm/sec	6.7(4.8 – 12.5)	3.2(2.96 – 3.73)	-2.251	0.024*

PSV: peak systolic velocity, EDV: end-diastolic velocity, SV: stroke volume

Table 5: Comparison between different neurological lesions regarding MR-CSF Flowmetry

	NPH	Aqueduct stenosis	Atrophic changes	Other causes	T	p-value
	Mean ± SD	Mean ± SD	Mean ± SD	Mean ± SD		
Evan's index	0.37 ± 0.08	0.42 ± 0.1	0.34 ± 0.07	0.35 ± 0.05	4.878	0.181
	Median (IQR)	Median (IQR)	Median (IQR)	Median (IQR)	KW	p-value
PSV cm/sec	5.8 (3.94 - 8.12)	5.74 (4.7 - 9.5)	2.6 (1.28 - 4.63)	4.5 (3.9 - 5.87)	10.79	**0.013***
Pairwise	P_1 0.487	**P_2 0.003***	P_3 0.228	**P_4 0.007***	P_5 0.47	P_6 0.238
EDV cm/sec	6.16 (3.25 - 8.05)	6.7 (4.8 - 12.5)	2.8 (1.63 - 4.8)	5.4 (4.8 - 6.75)	7.164	0.067
SV µL /cycle	92 (53 - 101.5)	107 (93 - 137)	35.5 (28 - 38.25)	54 (49 - 62)	18.969	**<0.001****
Pairwise	P_1 0.237	**P_2 0.001****	P_3 0.234	**P_4 0.001****	P_5 0.252	P_6 0.054

KW Kruskal Wallis test, F One-way ANOVA test. *p<0.05 is statistically significant. p1 difference between the aqueduct stenosis group and the NPH group. p2 difference between atrophic and aqueductal groups. P3 difference between atrophic changes and other neurological lesions. p4 difference between atrophic changes and NPH groups. P5 difference between NPH and other neurological lesions. p6 difference between aqueduct stenosis and other neurological changes. PSV: peak systolic velocity, EDV: end-diastolic velocity, SV: stroke volume

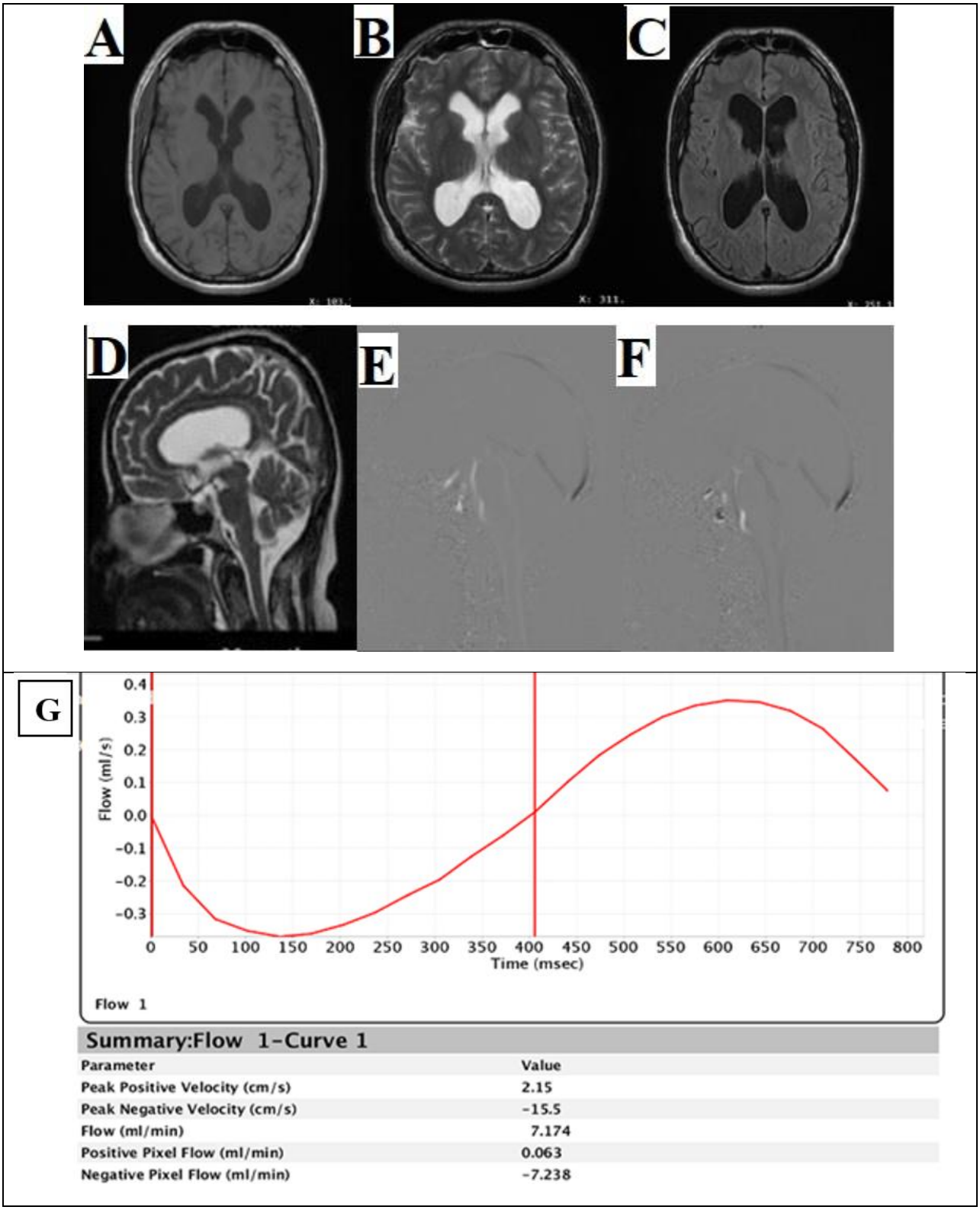

Summary:Flow 1-Curve 1

Parameter	Value
Peak Positive Velocity (cm/s)	2.15
Peak Negative Velocity (cm/s)	-15.5
Flow (ml/min)	7.174
Positive Pixel Flow (ml/min)	0.063
Negative Pixel Flow (ml/min)	-7.238

Figure 1: (A-D) Conventional MRI findings: Baseline MRI study including (A) axial T1, (B) Axial T2, (C) axial Flair, and (D) sagittal T2 show: Dilatation in whole ventricular system with Evans index = 0.39. There are no abnormal signal or space-occupying lesions in either cerebral hemispheres. No displacement of cerebellar

tonsils. (E-G) CSF Flowmetry study (GE machine): Qualitative assessment: Sagittal phase contrast images (E, F) show a high signal in diastole (appeared as shades of white) and a low signal in systole (appeared as dark shades). Quantitative measurements: Velocity-time curve (G) shows CSF in both diastoles (above the baseline curve) and systole (below the baseline). CSF systolic cycle duration is about 370 msec. Stroke volume =Mean systolic flow x duration of cardiac cycle =7.174 /24 x 370 =107.3 microliter/cycle. This finding is consistent with hyperdynamic CSF circulation. Clinical findings, conventional MR, and CSF flowmetry studies confirm a diagnosis of normal pressure hydrocephalus.

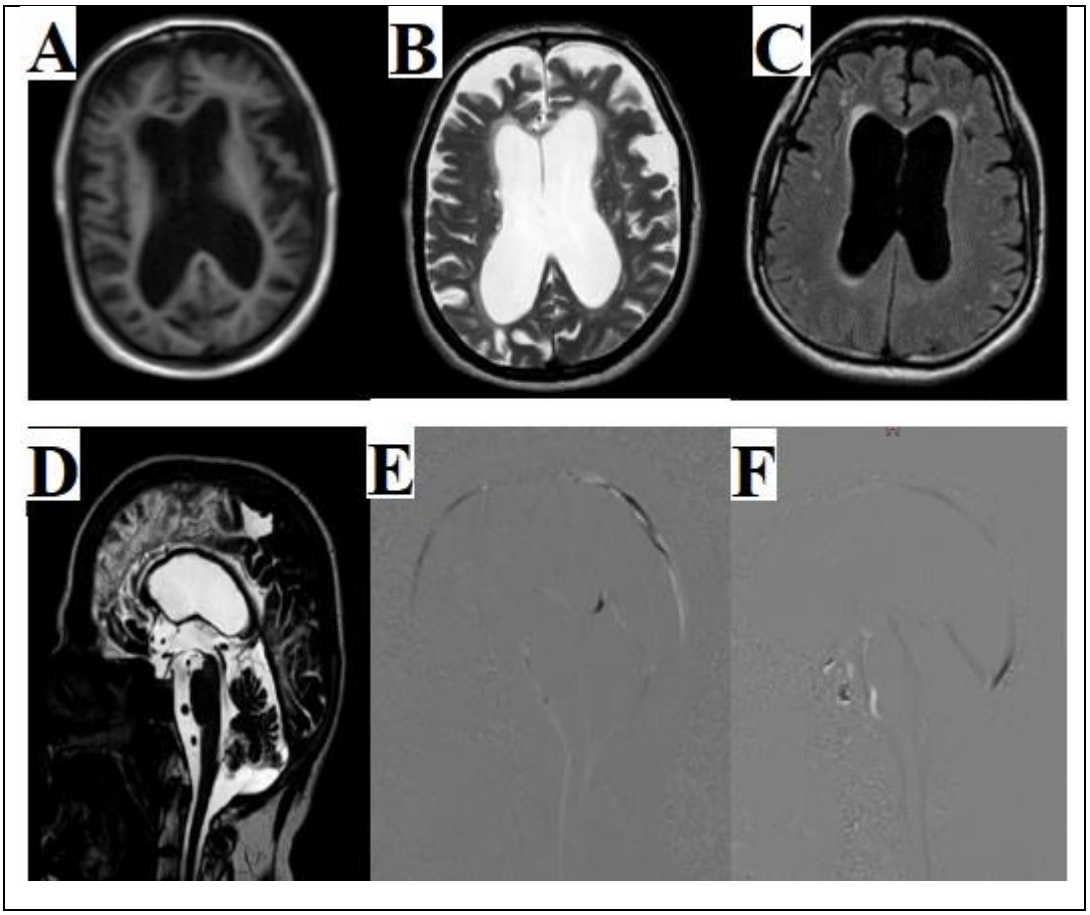

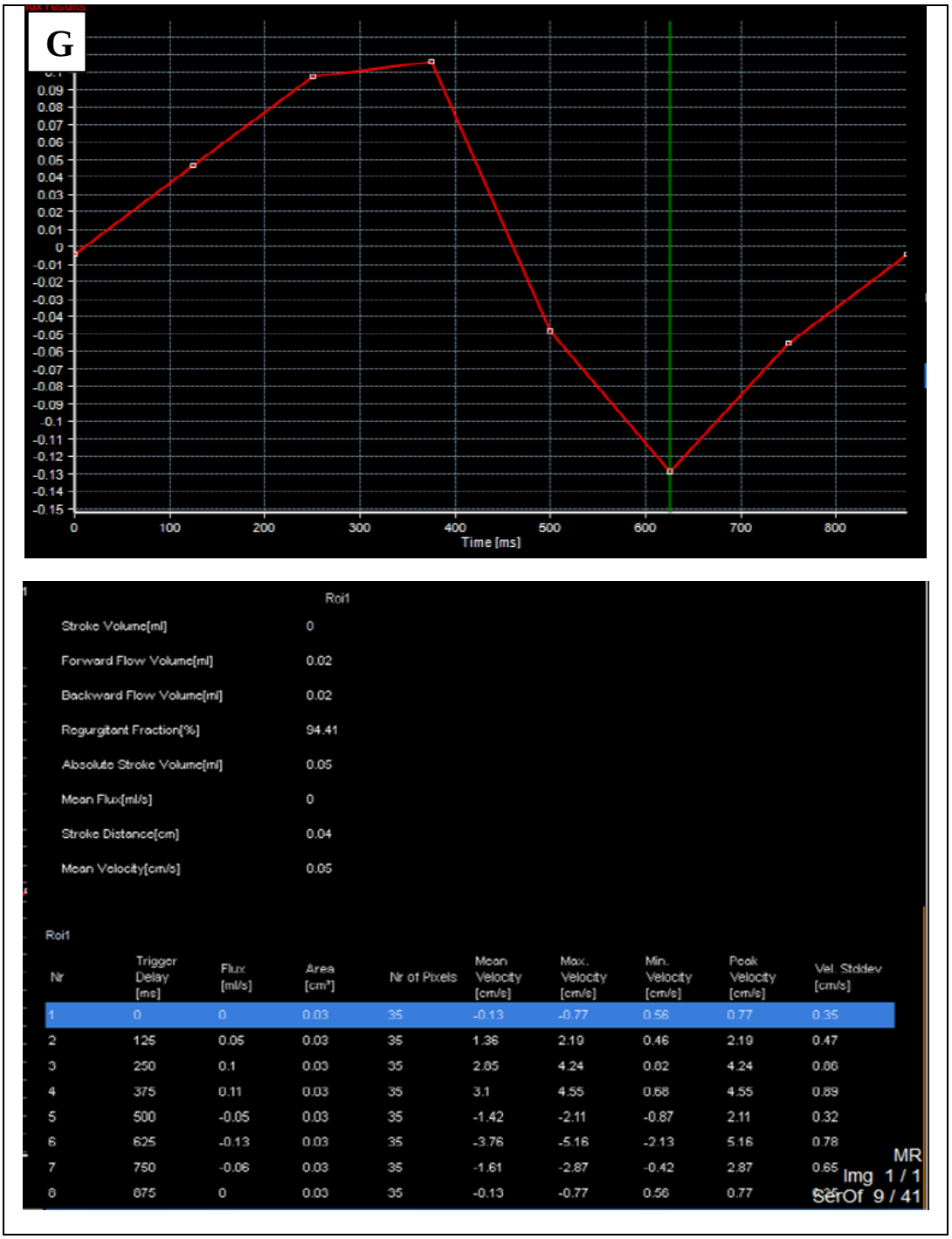

Figure 2: (A-D) Conventional MRI findings: Baseline MRI study including (A) axial T1, (B) Axial T2, (C) axial Flair, and (D) sagittal T2 show: Dilatation in whole ventricular system with Evans index = 0.35. There are no abnormal signal or space-occupying lesions in either cerebral hemispheres. No displacement of cerebellar tonsils. (E-G) CSF Flowmetry study (Philips machine): Qualitative assessment: Sagittal phase contrast images (E, F) show a high signal in diastole (appeared as shades of white) and a low signal in systole (appeared as dark shades). Quantitative measurements: Velocity-time curve (G) shows CSF in both diastoles (above the baseline baseline curve) and systole (below the baseline). CSF systolic cycle duration is about 430 msec. forward flow volume = 0.02 x 1000 = 20 microliter, backward flow volume = 0.02 x 1000 = 20 microliter and the

stroke volume = (20+20)/2 = 20 microliter/cycle. This finding is consistent with hypodynamic CSF circulation. Clinical findings, conventional MR, and CSF flowmetry studies confirm a diagnosis of brain atrophy.

DISCUSSION

This study included 46 cases: 36 patients with clinically suspected hydrocephalus or proved to have ventriculomegaly due to CSF abnormalities and another 10 control cases free from neurological lesions. Our findings regarding neurological lesions were similar to those of Hussein et al. [6], in which patients with various neurological lesions were included. However, in our study, we included an additional group of patients with vasodilatation due to treated tumors.

Conventional MRI findings in patients with NPH agreed with Hashimoto et al. [8], who reported MRI findings of enlarged Sylvian fissure with ventriculomegaly as disproportionately enlarged subarachnoid space in such patients. Patients with brain atrophy had prominent cortical sulci, basal cisterns, both Sylvian fissures, and extra-axial CSF spaces associated with ventricular system dilatation. This was similar to previous reports by Shmidt et al. [9] and Drayer et al. [10], in which findings of ventricular dilatation and dilatation in sulci as a result of cortical atrophy were also noted on conventional MRI.

Patients with Chiari Malformation type I showed downward displacement of the cerebellar tonsils to become pointed more than rounded. Korbecki et al. [11] observed similar findings in their study, and a diagnosis of CM type I was made when a descent of the cerebellar tonsil 5 mm below the McRae line was observed. Patients with aqueductal stenosis showed conventional MRI features of obstructive hydrocephalus in the form of supratentorial hydrocephalus (enlargement of both lateral ventricle and 3rd ventricle with relatively normal size fourth ventricle) and aqueductal flow void sign / aqueductal web. This agreed with Stoquart-El Sankari et al. [12], who reported MRI findings of triventricular dilatation with a comparatively small fourth ventricle and direct visibility of signal void sign at the aqueductal level.

Patients with a previous VP shunt operation showed ventricular dilatation by conventional MRI, which agreed with Sivaganesan et al. [13], who demonstrated one of the MRI findings of VP shunt is ventricular dilatation. Patients presenting with operated tumors had post-operative conventional MRI changes of vasodilatation of the ipsilateral ventricle. Similar MRI findings were reported by Kartal MG et al. [14]. However, we did not find any features of obstructive hydrocephalus reported by Kartal MG et al. [14] as symmetrical widening between the lateral ventricle and the 3rd ventricle, but in our study, only evacodilatation of the ipsilateral ventricle was seen on MRI.

In our investigation, the three primary quantitative CSF flowmetry parameters used to identify CSF flow dynamics through the Sylvius aqueduct were the peak diastolic and systolic velocities, both measured in centimeters/second, which were derived from the mean velocity-time curve. Moreover, the stroke volume, measured in microliters (µL) per cycle, is the average of the CSF volume flowing through the aqueduct during the systole and diastole.

Our findings regarding the quantitative evaluation of CSF flowmetry agreed with Abdelhameed et al. [1], who also found no gender predilection in their control group. Our study also showed no significant difference among younger and older age groups for Evan's index or any other (PSV, EDV, & SV) flowmetry parameters (all p-values >0.05). However, we did notice higher stroke volumes in the younger age group. In the control group, we obtained a mean stroke volume of 25.3±3.56 µL/cycle in the younger age group (11 to 20 years), which is in close agreement with Schroder et al. [15], who revealed a stroke volume of 28 µL/cycle in a normal individual. In the old age group (37 to 64 years), the mean stroke volume was about 20.0 ± 3.16 µL/cycle, which is in close accordance with Abbey et al. [16], who showed a stroke volume of 17.4 ±10.11 µL/cycle in normal individuals. This difference was likely due to differences among age groups in both studies [15,16].

In 36 patients with various neurologic disorders in our study, Quantitative measurements showing hyperdynamic CSF flow in all NPH cases were found to be considerably greater in the NPH group when compared to the control group. These results were also similar to those of Giner et al. [17], who found that there was a substantial elevation in PSV and EDV in NPH cases compared with the control group. This also agreed with previous investigations by Abdallah et al. [18], Baker et al. [19], and Youssef et al. [20] that also found a substantially increased mean PSV and aqueductal stroke volume (SV) among NPH patients. Our study showed a

significant difference between NPH and control groups with regards to Evan's index, SV, PSV, and EDV ($p<0.05$) that keeps with findings by Kahlon B et al. [21], who reported similar statistical differences between the NPH group and control groups. On the other hand, quantitative assessment in patients with brain atrophy showed a statistically significant difference in comparison to the control group regarding stroke volume (p-value<0.001). Still, it indicated hyperdynamic flow in comparison to SV of another neurological disease. This agrees with the findings by Hussein et al. [6], in which lower PSV and EDV were also reported.

Quantitative assessment to further localize the site of obstruction in 7 cases with findings of obstructive hydrocephalus by conventional MRI found a remarkable variation between aqueductal stenosis and control groups. All values, namely Evan's index, SV, PSV, and EDV, were notably increased in the aqueduct stenosis group ($p<0.05$). The combination of conventional MRI, 3D DRIVE sequence, and quantitative flow analysis through the aqueduct showed irregular CSF flow curves, as reported by Michali-Stolarska et al. [22], who similarly found curve irregularities in cases of obstruction. Furthermore, the mean stroke volume in our study was about 117.43 µL /cycle, indicating hyperdynamic CSF circulation. This agrees with Parkkola et al. [23], who reported the patients with aqueductal stenosis and hyperdynamic aqueductal flow.

The final two patients presenting with evacodilatation due to treated tumor showed a significant increase in Evan's index, PSV, and SV, similar to Eslamian et al. [24], were elevated quantitative PC MRI predicting the presence of hydrocephalus after the operated tumor. This also agreed with Mohammad et al. [25], who showed quantitative parameter elevation on CSF flowmetry but differed in age group and pre-to post-operative status.

So, to summarize our quantitative flowmetry findings with regards to stroke volume (SV) and its relation to the pathophysiological pattern of the studied group, we found physiological causes to include brain atrophy as hyperdynamic flow and NPH as a hyperdynamic flow that agrees with previously reported studies [6,18,20]. Other pathologically different neurological lesions including aqueductal stenosis, Chiari malformation type I, and evacodilatation of treated tumor showed hyperdynamic flow that is in keeping with most of the previous reported studies [11,22,24,26].

Our main quantitative finding was that an aqueductal SV above 44.5 microliter/ cycle of patients of NPH was found to have an area under the curve 0.923 with a diagnostic accuracy of about 91.3% (p value<0.001). This is considered a confirmation of hyperdynamic circulation and can be used as a cutoff to predict shunt responsiveness.

During clinical follow-ups of NPH patients, we found that 11 out of 13 patients had a good response to VP shunt surgery with improvement of the clinical symptoms. These patients had mean SV above 44.5 µL /cycle. The remaining two patients with shunt non-responsiveness cases had mean SV below 40 µL /cycle. This further emphasizes that a cutoff aqueductal SV above 44.5 µL /cycle is a valuable predictor of favorable outcomes after shunt operation. Yet, mild hyperdynamic CSF circulation values are still not an absolute exclusion criterion for VP shunt operation. In this case, the VP shunt may not be the preferred option as the patient is less likely to respond to the shunt. These findings match those previously reported by Senger et al. [27], who reported that patients with higher stroke volumes were shown to have better VP shunt placement. Nevertheless, we did define a slightly higher cutoff stroke volume (44.5 µL /cycle) in our study than that (42 µL /cycle) defined by Senger et al. [27].

There were some limitations in our study, as follows: all measurements were done once without serial assessments despite the clinical follow-up of some patients. The small sample size that was further subdivided into smaller groups, the relatively smaller number of the participants from the pediatric age group due to refusal to give consent, and some technical problems such as the modification of VENC (velocity encoding) in some cases, multiple trials to achieve an accurate VENC, and the time-consuming nature of this process added to the difficult of obtaining some results. We recommend the use of phase contrast MRI in patients with clinical suspicion of NPH to confirm the diagnosis and differentiate it from atrophic changes, as well as evaluation of different neurological diseases and follow-up after surgery. In NPH patients who are candidates to undergo ventriculoperitoneal shunt, preprocedural calculation of systolic stroke volume can help guide patient management and prognosis.

CONCLUSION

Through the study of our cases, we concluded that MRI CSF flowmetry provides an easy, safe, and non-invasive method for the diagnosis of different causes of ventriculomegaly/hydrocephalus. CSF flowmetry is a reliable and comprehensive imaging technique for the localization of level of obstruction, differentiation between brain atrophic changes and NPH, evaluation of VP shunt function and shunt responsiveness, and objective follow-up of different neurological diseases due to its high predictive value by which we can evaluate clinical course before and after surgery.

Conflict of interest: None
Financial Disclosure: None

REFERENCES

1. Abdelhameed AM, Darweesh EAF, Bedair MH. Role of MRI CSF Flowmetry in Evaluation of Hydrocephalus in Pediatric Patients. The Egyptian Journal of Hospital Medicine. 2017;68:1291–6.
2. Verrees M, Selman WR. Management of normal pressure hydrocephalus. I am Fam Physician. 2004;70:1071–8.
3. Gandhoke GS, Frassanito P, Chandra N, Ojha BK, Singh A. Role of magnetic resonance ventriculography in multiloculated hydrocephalus: Clinical article. PED. 2013;11:697–703.
4. Igra MS, Romanowski CAJ, Stivaros SM. Imaging of CSF Spaces: Anatomy, Physiology, and Hydrodynamics. In: Barkhof F, Jäger HR, Thurnher MM, Rovira À, editors. Clinical Neuroradiology: The ESNR Textbook [Internet]. Cham: Springer International Publishing; 2019 [cited 2024 Jan 3]. p. 431–49. Available from: https://doi.org/10.1007/978-3-319-68536-6_5
5. DANDY WE, BLACKFAN KD. AN EXPERIMENTAL, CLINICAL AND PATHOLOGICAL STUDY: Part 1.—Experimental Studies. American Journal of Diseases of Children. 1914;VIII:406–82.
6. Hussein, Mostafa M. Magdy MD, Gamal El-Din MD. Prognostic Value of MRI-CSF Flowmetry for Shunt Responsiveness in Patients with Idiopathic Normal Pressure Hydrocephalus. The Medical Journal of Cairo University. 2022;90:403–8.
7. Elsafty HG, ELAggan AM, Yousef MA, Badawy ME. Cerebrospinal fluid flowmetry using phase-contrast MRI technique and its clinical applications. Tanta Medical Journal. 2018;46:121.
8. Hashimoto M, Ishikawa M, Mori E, Kuwana N, Study of INPH on neurological improvement (SINPHONI). Diagnosis of idiopathic normal pressure hydrocephalus is supported by MRI-based scheme: a prospective cohort study. Cerebrospinal Fluid Res. 2010;7:18.
9. Schmidt R, Launer L, Nilsson L. Magnetic resonance imaging of the brain in diabetes: cortical atrophy was associated with diabetes. Diabetes. 2004;53:687–92.
10. Drayer BP. Imaging of the aging brain. Part I. Normal findings. Radiology. 1988;166:785–96.
11. Korbecki A, Zimny A, Podgórski P, Sąsiadek M, Bladowska J. Imaging of cerebrospinal fluid flow: fundamentals, techniques, and clinical applications of phase-contrast magnetic resonance imaging. Polish journal of radiology. 2019;84:240–50.
12. Stoquart-El Sankari S, Lehmann P, Gondry-Jouet C, Fichten A, Godefroy O, Meyer M-E, et al. Phase-contrast MR imaging support for the diagnosis of aqueductal stenosis. American Journal of Neuroradiology. 2009;30:209–14.
13. Sivaganesan A, Krishnamurthy R, Sahni D, Viswanathan C. Neuroimaging of ventriculoperitoneal shunt complications in children. Pediatric radiology. 2012;42:1029–46.
14. Kartal MG, Algin O. Evaluation of hydrocephalus and other cerebrospinal fluid disorders with MRI: An update. Insights into imaging. 2014;5:531–41.
15. Schroeder HW, Schweim C, Schweim KH, Gaab MR. Analysis of aqueductal cerebrospinal fluid flow after endoscopic aqueductoplasty by using cine phase-contrast magnetic resonance imaging. Neurosurgical Focus. 2000;9:1–8.
16. Abbey P, Singh P, Khandelwal N, Mukherjee K. Shunt surgery effects on cerebrospinal fluid flow across the aqueduct of Sylvius in patients with communicating hydrocephalus. Journal of Clinical Neuroscience. 2009;16:514–8.
17. Giner JF, Sanz-Requena R, Flórez N, Alberich-Bayarri A, Garcia-Marti G, Ponz A, et al. Quantitative phase-contrast MRI study of cerebrospinal fluid flow: a method for identifying patients with normal-pressure hydrocephalus. Neurología (English Edition). 2014;29:68–75.
18. Abdallah A, Shabaan M, Hassan M, Yassin A. The role of MRI-CSF flowmetry in differentiation between NPH and involutional brain changes. European Congress of Radiology-ECR; 2015.
19. Baker II, El Sayed NM, Atta YA. Brain atrophy versus normal pressure hydrocephalus by CSF flow measurement at MRI; 2009.

20. Youssef A, Magdy AM, Abdul-Rahman AA-A. The role of MRI-CSF flowmetry in the diagnosis of idiopathic normal pressure hydrocephalus. Fayoum University Medical Journal. 2021;8:19–30.
21. Kahlon B, Annertz M, Ståhlberg F, Rehncrona S. Is aqueductal stroke volume, measured with cine phase-contrast magnetic resonance imaging scans useful in predicting outcome of shunt surgery in suspected normal pressure hydrocephalus? Neurosurgery. 2007;60:124–30.
22. Michali-Stolarska M, Bladowska J, Stolarski M, Sąsiadek MJ. Diagnostic imaging and clinical features of intracranial hypotension: review of literature. Polish Journal of Radiology. 2018;83.
23. Parkkola R, Komu M, Äärimaa T, Alanen M, Thomsen C. Cerebrospinal fluid flow in children with normal and dilated ventricles studied by MR imaging. Acta radiologica. 2001;42:33–8.
24. Eslamian M, Habibi Z, Kankam SB, Khoshnevisan A. Role of CSF flow parameters in diagnosis and management of persistent post-operative hydrocephalus. Interdisciplinary Neurosurgery. 2022;30:101634.
25. Mohammad SA, Osman NM, Ahmed KA. The value of CSF flow studies in the management of CSF disorders in children: a pictorial review. Insights into imaging. 2019;10:1–13.
26. Raybaud C. MR assessment of pediatric hydrocephalus: a road map. Child's Nervous System. 2016;32:19–41.
27. Senger KPS, Singh RK, Singh AK, Singh A, Dashottar S, Sharma V, et al. CSF flowmetry: an innovative technique in diagnosing normal pressure hydrocephalus. International Journal of Advances in Medicine. 2017;4:682–7.

Citation

Helmy, N., Hafez, F., Zaitoun, M., Dessouky, R. Role of MR-CSF Flowmetry in Diagnosis and Differentiation of ventriculomegaly. *Zagazig University Medical Journal*, 2024; (3937-3952): -. doi: 10.21608/zumj.2024.262202.3110

Table S1: clinical data of patient group

Clinical presentation:		
Headache	26	72.2%
Signs of ICT	25	69.4%
Gait disturbance	18	50%
Dementia	15	41.7%
Urine incontinence	11	30.6%
Delayed development (motor or mental)	4	11.1%
Comorbidities:		
Hypertension	2	5.6%
Diabetes, hypertension	1	2.8%
Past history:		
Old infarction	3	8.3%
Old tumor	2	5.6%
VP shunt	2	5.6%
Trauma	1	2.8%

Table S2: Atrophic changes regarding gender and clinical data

Gender:		
Female	6	60%
Male	4	40%
Dementia	10	100%
Headache	8	80%
Signs of ICT	8	80%
Gait disturbance	3	30%
Urine incontinence	2	20%
Delayed mental development	1	10%
Comorbidities:		
Hypertension	1	10%
Diabetes, Hypertension	0	0%
Past history		
Old lacunar infarction	1	10%
Trauma	0	0%

Table S3: NPH regarding gender & clinical data

Gender:		
Male	8	61.5 %
Female	5	38.5 %
Dementia	13	100%
Gait disturbance	13	100%
Headache	10	76.9%
Urine incontinence	9	69.2%
Signs of ICT	4	30.8 %

Delayed mental development	0	0%
Comorbidities:		
Diabetes, hypertension	0	0%
Hypertension	0	0%
Past history		
Old lacunar infarction	1	7.7%
Trauma	0	0%

Table S4: Distribution of patients according to Stroke volume and pathophysiology

Physiological causes:			
Hypodynamic: **Atrophic changes**	10	21 %	35.5 ± 7.83
Hyperdynamic: **NPH**	13	28.3%	84.38 ± 33.48
Pathological causes:			
Hyperdynamic: **Aqueductal stenosis**			
Chiari Malformation Type I	7	15.2%	117.43 ± 51.82
Therapeutic tumor (vasodilatation of treated SOL)	2	4.3%	45 ± 6.83
	2	4.3%	47 ± 6.83

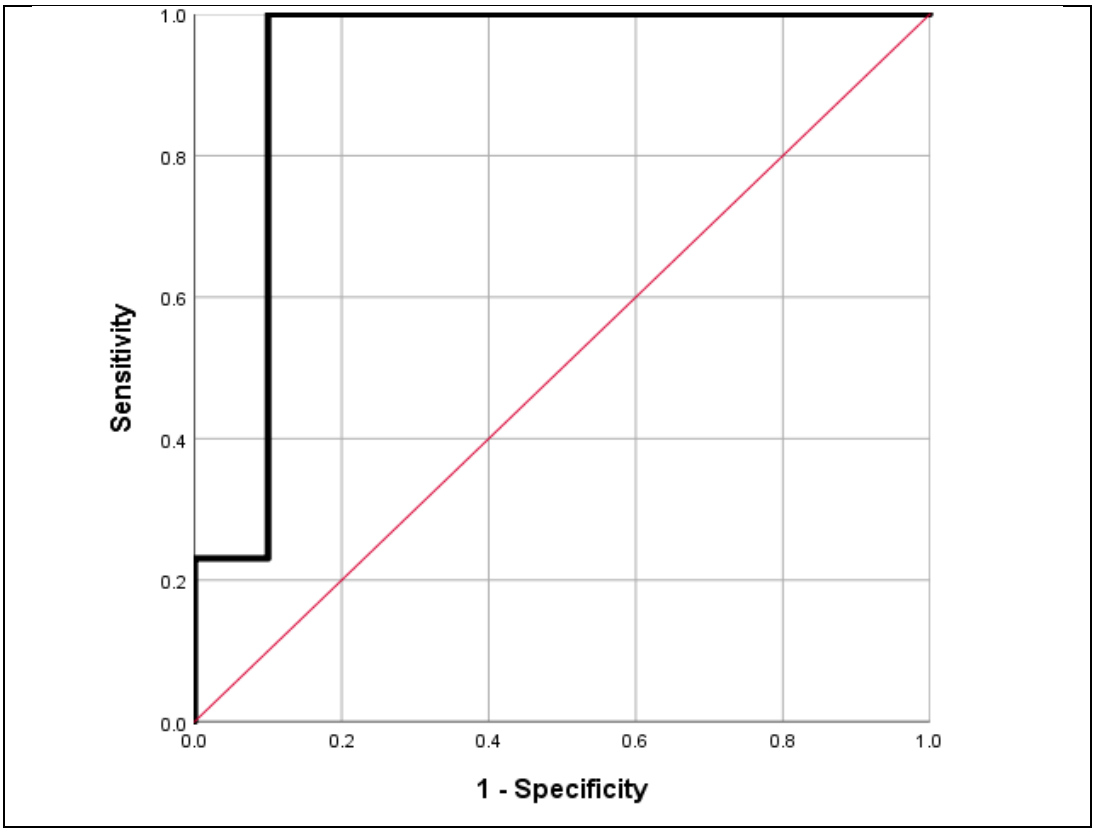

Figure S1: ROC curve showing performance of SV in the diagnosis of atrophic changes (versus) NPH among the studied patients